



Contents lists available at ScienceDirect

# Spectrochimica Acta Part A: Molecular and Biomolecular Spectroscopy

journal homepage: [www.journals.elsevier.com/spectrochimica-acta-part-a-molecular-and-biomolecular-spectroscopy](http://www.journals.elsevier.com/spectrochimica-acta-part-a-molecular-and-biomolecular-spectroscopy)

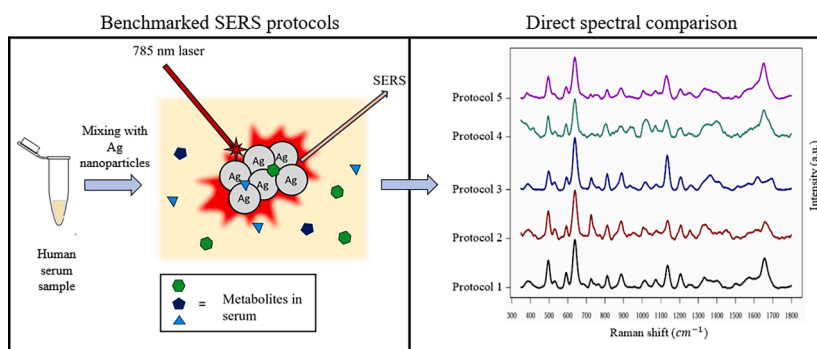
## Direct comparison of different protocols to obtain surface enhanced Raman spectra of human serum

Roberto Gobatto<sup>a</sup>, Stefano Fornasaro<sup>b</sup>, Valter Sergio<sup>a</sup>, Alois Bonifacio<sup>a,\*</sup><sup>a</sup> Raman Spectroscopy Laboratory, Department of Engineering and Architecture, University of Trieste, Via Valerio 6a, 34127 Trieste, TS, Italy<sup>b</sup> Department of Chemical and Pharmaceutical Sciences, University of Trieste, Via Licio Giorgieri 1, 34127 Trieste, TS, Italy

## HIGHLIGHTS

- Surface enhanced Raman Spectroscopy (SERS) spectra of human serum with different protocols are reported.
- Five different protocols for serum analysis are compared for a better benchmarking and standardization.
- All protocols yield the similar spectra, but they differ in terms of spectral intensity, repeatability, and preparation steps.
- All protocols yield the same biochemical information, mostly about uric acid and hypoxanthine.

## GRAPHICAL ABSTRACT



## ARTICLE INFO

## Keywords:

SERS  
Serum  
Protocols  
Biofluids  
Silver nanoparticles  
Uric acid

## ABSTRACT

Label-free Surface Enhanced Raman Spectroscopy (SERS) is a rapid technique that has been extensively applied in clinical diagnosis and biomedicine for the analysis of biofluids. The purpose of this approach relies on the ability to detect specific “metabolic fingerprints” of complex biological samples, but the full potential of this technique in diagnostics is yet to be exploited, mainly because of the lack of common analytical protocols for sample preparation and analysis. Variation of experimental parameters, such as substrate type, laser wavelength and sample processing can greatly influence spectral patterns, making results from different research groups difficult to compare. This study aims at making a step toward a standardization of the protocols in the analysis of human serum samples with Ag nanoparticles, by directly comparing the SERS spectra obtained from five different methods in which parameters like laser power, nanoparticle concentration, incubation/deproteinization steps and type of substrate used vary. Two protocols are the most used in the literature, and the other three are “in-house” protocols proposed by our group; all of them are employed to analyze the same human serum sample. The experimental results show that all protocols yield spectra that share the same overall spectral pattern, conveying the same biochemical information, but they significantly differ in terms of overall spectral intensity, repeatability, and preparation steps of the sample. A Principal Component Analysis (PCA) was performed revealing that protocol 3 and protocol 1 have the least variability in the dataset, while protocol 2 and 4 are the least repeatable.

\* Corresponding author.

E-mail addresses: [roberto.gobatto@phd.units.it](mailto:roberto.gobatto@phd.units.it) (R. Gobatto), [sfornasaro@units.it](mailto:sfornasaro@units.it) (S. Fornasaro), [sergo@units.it](mailto:sergo@units.it) (V. Sergio), [abonifacio@units.it](mailto:abonifacio@units.it) (A. Bonifacio).<https://doi.org/10.1016/j.saa.2024.124390>

Received 12 March 2024; Received in revised form 21 April 2024; Accepted 29 April 2024

Available online 30 April 2024

1386-1425/© 2024 The Authors. Published by Elsevier B.V. This is an open access article under the CC BY license (<http://creativecommons.org/licenses/by/4.0/>).

## 1. Introduction

Surface-enhanced Raman spectroscopy (SERS) [1] relies on the amplification of Raman scattering by nanostructured metal surfaces with adequate plasmonic properties. In the last decade, SERS has increasingly been used for the direct, untargeted analysis of serum, as well as other biofluids, to classify samples with the aim of diagnosing a variety of diseases [2,3]. The underlying assumption of all these research efforts is that some of the metabolic differences in serum due to a pathological state can be detected by SERS. The direct SERS analysis of a biochemically complex biofluids, such as serum, is experimentally challenging because they are constituted by more than thousands of metabolites [4], various proteins and electrolytes, plus minor amounts of other species (e.g., circulating nucleic acids, exosomes, etc.). Specifically, the high amount of proteins can potentially interfere with the spectroscopic detection of metabolites, since proteins are known to rapidly adsorb on surfaces (i.e., “protein fouling”), including metal surfaces like those used as SERS substrates. Moreover, the formation of a protein layer (i.e., “protein corona”) on the surface of nanoparticles, including the Ag and Au ones commonly used as metal substrates in SERS, is known to inhibit nanoparticles aggregation, and thus the formation of the inter-particle gaps (i.e., “hot spots”) essential for SERS [1].

In the absence of a standard methodology for SERS analysis of serum, different approaches were used by different research groups, involving various metal substrates, sample pre-treatments, and preparation protocols. Despite the diversity of the protocols used, the results obtained are loosely comparable in terms of the overall spectral profile, i.e., the position of the bands observed and their relative intensities. A survey on literature shows that relatively few research groups are responsible for most of the studies using SERS on serum, and that a set of protocols recurs in many studies, emerging as the most common. In particular, protocols using Ag colloids as substrates and an excitation at 785 nm are recurrent in most of the available studies. The main differences among protocols are the physical state (liquid or solid) of the sample to be measured (e.g., the presence of a drying step), the use of Ag nanoparticles in their colloidal form or deposited on solid supports as solid substrates (e.g., paper), and the presence of a de-proteinization step or a

prolonged incubation of serum with the substrate.

Considering the growing importance that the direct untargeted SERS analysis of serum is gaining in recent years, as well as the absence of a benchmark, a critical comparison among different protocols, focusing on highlighting the specificities of each method, would be desirable. Such a comparison might guide researchers approaching SERS of serum in selecting their own method, and it will facilitate the critical assessment of results obtained by different research groups.

The aim of this study is to partially fill this gap by directly comparing five protocols sharing the use of Ag colloids and an excitation at 785 nm for the SERS analysis of human serum. The set includes two protocols which are frequently used in the literature by various research groups, as well as three protocols developed by our group and described in previous publications. Details about these protocols can be found in the Materials and Methods section and are summarized in Fig. 1 and in Table 1. As previously stated, all these protocols use Ag colloids, a very common and easily made SERS substrate, as well as a widespread excitation wavelength, making results easily reproducible by others. Differences among various protocols were evaluated in terms of overall intensity, spectral profile and its repeatability, using the same sample (a single batch of commercial human serum), the same Ag colloid (obtained by pooling different batches), the same instrument and the same operator.

## 2. Materials and methods

### 2.1. Literature survey

Protocols 1–5 were identified with a literature search in the SCOPUS database using as query: (“SERS” OR “surface enhanced Raman”) AND “Serum” AND (“diagnosis” OR “classification”) for papers published from 2015 to 2023. Only papers reporting at least one SERS spectrum obtained with a direct untargeted detection strategy (i.e. without the use of labels or reporters) were considered.

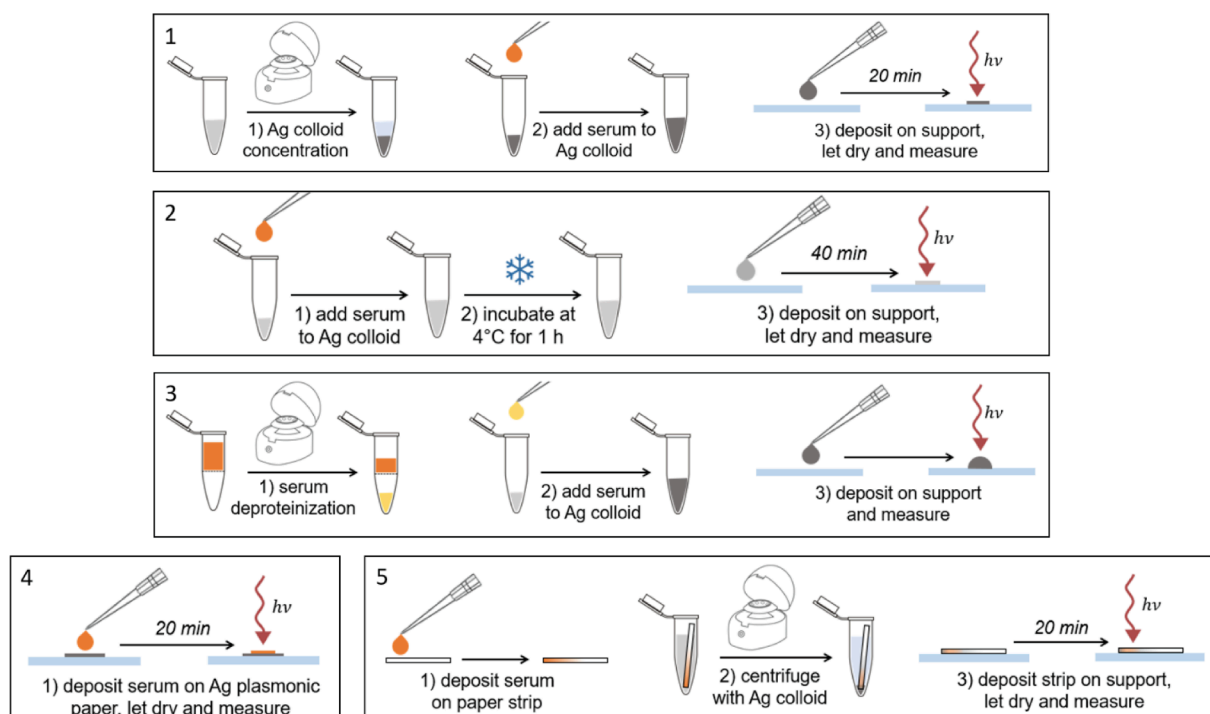


Fig. 1. Graphical representation of steps involved in the different protocols (1–5) used in this study.

## 2.2. Reagents and solvents

Analytical grade silver nitrate, sodium citrate tribasic, hydroxylamine hydrochloride, and sodium hydroxide (reagent grade >98 %, anhydrous) used for the nanoparticle synthesis were purchased from Merck. Nitric acid (>65 %) and NoChromix® used for glassware cleaning were purchased by Merck. Commercially available Vivaspin® ultrafiltration spin columns with a molecular weight cut-off of 3 kDa (Sartorius), and qualitative filter papers with particle retention of 2 µm (VWR-Avantor) were employed. UV-grade calcium fluoride (CaF<sub>2</sub>) slides were purchased from Crystal GmbH. Pure ethanol (>99.8 %, Sigma-Aldrich) and ultrapure milliQ water were used to clean the CaF<sub>2</sub> slides.

## 2.3. Human serum

Three different commercial human serum batches (from male AB clotted whole blood, USA origin, sterile filtered) were purchased from Merck (product number H6914) and then pooled to create a single reference batch. The final serum batch was then aliquoted in 2 mL Eppendorfs and frozen at -30 °C to prevent degradation over time.

## 2.4. Citrate-reduced Ag colloid preparation

All the protocols presented in this study used Ag nanoparticles that were prepared via the sodium citrate reduction method known also as Lee-Meisel synthesis [5]. Before starting the synthesis procedure, all glassware was accurately washed sequentially with NoChromix® solution, milliQ water, nitric acid and again with milliQ water. The cleaning step is fundamental to eliminate metal and organic contaminants from the surfaces of the glassware that could interfere with the nanoparticles synthesis. Briefly, 90 mg of silver nitrate were added to 500 mL of milliQ water contained in a two-neck 1000 mL Erlenmeyer flask. The Erlenmeyer was then linked to an Allihn condenser, put on a heating plate, and the solution was homogeneously stirred until boiling. Subsequently, 10 mL of sodium citrate tribasic solution 1.1 % w/v were added dropwise. The solution turned from transparent to grey within few minutes after the addition of the citrate solution. The reaction mix was kept boiling for 1 h, and the container was wrapped with aluminium foil to protect it from light. After cooling the colloidal solution to room temperature, nanoparticles were ready for use and were stored in the dark for both colloidal SERS measurements, and for the preparation of SERS solid substrates.

The UV-Visible extinction spectra were collected with a Cary 60 UV-Vis Agilent Technologies diluting the colloidal solution 10 times in milliQ water and placing it in a 2.5 mL PMMA cuvette.

## 2.5. Hydroxylamine-reduced Ag colloid preparation

For protocol 1, some tests were conducted using hydroxylamine-

reduced Ag nanoparticles (see Section 2.6.1), which were synthesized in accordance with the Leopold-Lendl method [6]. A 4.5 mL sodium hydroxide solution 0.1 M was added to a 5 mL aqueous solution in which 0.021 g of hydroxylamine were previously dissolved. The resulting mixture was then added rapidly to a 90 mL silver nitrate 1.1 mM solution under vigorous stirring. The solution turned immediately from transparent to milky grey and stirring was maintained for 1 min. The obtained colloidal solution was stored in the dark, protected with aluminium foil and was stable up to 1 week.

UV-Visible extinction spectra were collected diluting the colloidal solution 10 times in milliQ water and placing it in a PMMA cuvette.

## 2.6. Protocols for SERS spectra acquisition

The protocols used in this study are summarized in Fig. 1 and Table 1 and are described in detail below. For all protocols, SERS measurements were performed with a B&W Tek i-Raman Plus portable system (BWS465-785S) connected to a compatible Raman microscope (BAC151B). The laser used was a CleanLaze® stabilized laser system model with a wavelength output of 785 nm and a maximum laser power of 400 mW. Sample illumination and scattered light collection was obtained using optical fibers connected to a compact microscope system mounting a 20 × Olympus objective (N.A. 0.4); the laser power, the number of accumulation and the time of exposure depend on the protocol used and are specified below. Since these parameters differed slightly among the papers considered as sources for protocol 1 and 2, the ones giving the best results with our instrument were selected for this study.

### 2.6.1. Protocol 1: concentrated dried Ag colloids

This protocol involves the analysis of serum mixed with concentrated Ag nanoparticles (in a 1:1 vol ratio), dried on a CaF<sub>2</sub> slide. First, 1 mL of Ag colloid was put in an Eppendorf and centrifuged for 15 min at a relative centrifugal force of 25,500g. The silver colloids were then concentrated 10 times by discarding 900 µL of the supernatant and resuspending the pellet in the remaining 100 µL solution. Serum sample was taken from the freezer at -30 °C and thawed in the fridge at 4 °C for 40 min. When the serum sample was completely melted, 5 µL were taken and mixed with 5 µL of concentrated Ag nanoparticles. Then, 5 µL of the mix were transferred onto a CaF<sub>2</sub> slide that had been previously cleaned with 2 washing steps of ethanol and milliQ water. The drop was left drying for exactly 20 min at room temperature, and then analysed with the Raman microscope. In some papers, before sample deposition and drying there is also an incubation step. However, we found no differences in spectra obtained with or without this step (data not shown), so we decided not to include it in this version of the protocol. The laser power was set to 10 mW, the integration time to 10 s with a single accumulation, and the measure was performed on the “coffee-ring” area of the drop in 5 different locations (see [Supplementary Material](#):

**Table 1**

Main characteristics of the protocols 1–5 used in this study.

| Protocol | Substrate            | Deproteiniz. step | Sample preparation                                      | Incubation step | Drying step  | Overall time* | Laser power | Refs.   |
|----------|----------------------|-------------------|---|-----------------|--------------|---------------|-------------|---------|
| 1        | Ag colloid (conc.)   | No                | Ag colloid + serum mixing (1:1 vol.ratio)               | No              | Yes (20 min) | 20 min        | 10 mW       | [10–23] |
| 2        | Ag colloid           | No                | Ag colloid + serum mixing (1:1 vol ratio)               | Yes (1 h, 4 °C) | Yes (40 min) | 100 min       | 100 mW      | [24–30] |
| 3        | Ag colloid           | Yes (40 min)      | Ag colloid + serum mixing (9:1 vol ratio)               | No              | No           | 40 min        | 180 mW      | [7,31]  |
| 4        | Plasmonic paper (Ag) | No                | Serum deposition on substrate                           | No              | Yes (20 min) | 20 min        | 20 mW       | [8,32]  |
| 5        | Ag colloid           | No                | Serum deposition on paper centrifug. With Ag colloids** | No              | Yes (20 min) | 40 min        | 35 mW       | [9]     |

\*Time needed to prepare sample for SERS spectral acquisition, starting with the whole serum and a substrate; measurement time and time needed to prepare the substrate are not considered.

\*\*First serum is deposited on paper, then added to colloid and centrifuged for 20 min.

Figure S1) This was done to evaluate the differences in the signal intensity of analytes from different dried zones of the sample. Moreover, to address protocol variability, spectra collection was done on 3 different replicates (i.e., 3 different dried drops) for a total of 15 spectra. Some of the papers applying this protocol use hydroxylamine-reduced Ag colloids [6] as substrates instead of citrate-reduced colloids. However, since hydroxylamine-reduced colloids are not stable for more than 1 week, whereas citrate-reduced Ag colloids are stable over a longer time, and since the two colloids give nearly identical spectra of serum in terms of overall intensity and spectral pattern (see [Supplementary Material: Figure S2](#)), citrate-reduced colloids were used.

#### 2.6.2. Protocol 2: non-concentrated dried Ag colloids

This protocol consists in the analysis of serum mixed with non-concentrated Ag nanoparticles (1:1 vol ratio), deposited and dried on a CaF<sub>2</sub> slide. Serum sample was taken from the freezer at -30 °C and thawed in the fridge at 4 °C for 40 min. When the serum was completely melted, 5 µL were taken and mixed with 5 µL of Ag nanoparticles. Then, the mix was incubated for 1 h at 4 °C in the fridge. After the incubation, 5 µL of the mix were transferred on a CaF<sub>2</sub> slide and the drop was left drying for 40 min at room temperature, then spectra were collected. The laser power was set to 100 mW, the integration time to 10 s with 3 accumulations; spectra were collected on the “coffee-ring” area of the drop in 5 different points (see [Supplementary Material: Figure S3](#)). As for Protocol 1, 15 spectra were recorded: 5 from 3 different replicates. The main differences with respect to protocol 1 were the use of non-concentrated Ag colloids, the additional incubation step at 4 °C and a higher laser power.

#### 2.6.3. Protocol 3: non-concentrated Ag colloids with deproteinized serum

This protocol [7] involves a de-proteinization step of the serum sample (via centrifugal filtration), followed by the addition of Ag colloid (1:9 vol ratio). A Vivaspin® ultrafiltration spin column with a molecular weight cut-off of 3 kDa (Sartorius) was filled with 500 µL of milliQ water and then centrifuged for 15 min at a relative centrifugal force of 25,500g. The filtered water was disposed, and the operation was repeated again for a second centrifugation cycle to eliminate all the glycerol in the filtration membrane. Serum sample was taken from the freezer at -30 °C and thawed in the fridge at 4 °C for 40 min, then 200 µL were put inside the spin column and the sample was centrifuged for 2 cycles for 20 min at a relative centrifugal force of 18,300g. Then, 5 µL of filtered serum were mixed with 45 µL of Ag colloid. The 50 µL mix was immediately put onto a glass slide covered with aluminium foil and then with a parafilm layer on top of it. The low wettability of the parafilm layer ensured a high contact angle between the drop and the substrate, keeping the liquid from spreading on the slide. The drop was analysed 5 min after it was placed on the slide with a laser power of 180 mW, setting the integration time to 10 s with 3 accumulations. The spectral collection was performed after focusing the laser on the top of the drop, so that Raman bands of the parafilm were not observed. The aggregation of the nanoparticles could be seen as a colour change in the drop that turned to a more blueish shading. The analysis was performed in the centre of 3 different drops (see [Supplementary Material: Figure S4](#)) with 5 successive spectra acquisitions for each drop, for a total of 15 spectra. This protocol is fundamentally different from protocols 1 and 2, as the analysis is performed on liquid samples, using de-proteinized serum.

#### 2.6.4. Protocol 4: Solid paper substrate with concentrated Ag nanoparticles

This protocol is based on the use of a solid SERS substrate obtained by the deposition of concentrated Ag nanoparticles on filter paper [8]. 36 falcons were filled with 10 mL solution of Ag nanoparticles and ultracentrifuged at a relative centrifugal force of 3800g for 1 h. 9 mL of the supernatant contained in each falcon were then discarded to obtain 1 mL of an Ag colloids solution concentrated 10 times. Squared-shaped 1 cm × 1 cm pieces of filter paper with particle retention of 2 µm (VWR-Avantor) were placed each inside a well in a 24 multi-well plastic plate.

Then, 3 mL of concentrated Ag colloid were gently piped inside each well. Subsequently, 62 µL of sodium citrate tribasic 1 M solution were piped and gently mixed inside each well. The solution turned colour from dark green to black due to nanoparticle aggregation. The multiwell was covered in aluminium foil and left to rest for 7 days. Then, the supernatant was removed, and the substrates were left to dry off for 12 h. Finally, the substrates were taken and stocked for months in milliQ water inside a multiwell or a Petri dish. Whenever a substrate was needed for SERS analysis, it was taken out of milliQ water and left to dry for 20 min above a sheet of blotting paper, then the substrate was cut in 9 smaller squares. In this operation particular attention must be taken in the manipulation of the substrates that must not fell upside down or damaged in the central part of the square. Serum sample was taken from the freezer at -30 °C and thawed in the fridge at 4 °C for 40 min, then 5 µL of the sample were pipetted on the Ag-paper substrate, which was then transferred onto an aluminium foil covered glass slide and left to dry for 20 min. Spectra were taken setting laser power to 20 mW, integration time 10 s with a single accumulation. To address protocol variability spectra collection was performed in 3 different replicates with 5 spectra acquisition for each substrate, for a total of 15 spectra (see [Supplementary Material: Figure S5](#)). This protocol is fundamentally different from the previous ones since it makes use of a solid substrate, in which Ag nanoparticles are already aggregated before adding the serum sample.

#### 2.6.5. Protocol 5: Centrifugal silver plasmonic paper (CSPP)

In this protocol [9] a small volume of serum is first added to the edge of a paper strip, and then the colloidal Ag nanoparticles are deposited on top of the paper by centrifugation. Filter paper with particle retention of 2 µm (VWR-Avantor) was cut in strips of 1.1 cm × 3 mm. Serum sample was taken from the freezer at -30 °C and thawed at 4 °C for 40 min, then 2 µL were put on the edge of the strip and left to dry for 4 min. The paper was then placed inside a 1,5 mL Eppendorf tube with 150 µL of Ag colloids; the side soaked with serum sample must face toward the bottom of the tube. The sample was centrifuged for 20 min at a relative centrifugal force of 9700g, and then the strip was gently taken out of the Eppendorf and left to dry above an aluminium foil-covered glass slide for 25 min. Spectra were then taken at 5 different positions in the paper surface near the edge of the strip on which previously serum had been spotted (see [Supplementary Material: Figure S6](#)) setting the laser power to 35 mW, integration time of 10 s with a single accumulation. To address protocol variability, spectra collection was done on 3 different paper strips with 5 spectra acquisitions for each substrate, for a total of 15 spectra. The distinctive characteristic of this protocol is that the addition of the Ag colloid is done on the dried serum on the paper strip.

### 2.7. Data pre-processing and visualization

All data analysis and visualization were made with the R software [33], using the “hyperSpec” package [34] to manage spectral data. A custom import function was used to import raw data (single.txt ASCII files) into a single hyperSpec S4 object containing all metadata. Spectral region was cropped for all spectra to 400–1800 cm<sup>-1</sup>. Baselines were calculated and subtracted for all spectra with the Asymmetric Least Squares (ALS) algorithm of the *baseline()* function (package “baseline” [35]), using the following parameters:  $\lambda = 4$ ,  $p = 0.005$ ,  $\text{maxit} = 100$ . Total intensity normalization was obtained by dividing each spectrum by a factor calculated as  $\sqrt{\sum(x_i^2)}$ , where  $x_i$  are the intensity values at each data point (vector normalization). PCA was done using the *prcomp()* function, centering but not scaling data. Figures were prepared using base R plotting functions.

## 3. Results and discussion

SERS spectra of human serum were detected with all the protocols used ([Fig. 1](#)). The obtained spectra were consistent with those reported

in literature for each protocol, with differences due to different serum samples, different instruments, and baseline subtraction algorithms. Spectra from all protocols shared the same fundamental pattern, with most bands having similar or even identical Raman shifts and comparable relative intensities. This similarity is consistent with the fact that all spectra were obtained with the same substrate (i.e., citrate-reduced Ag colloid) and the same extinction wavelength (i.e. 785 nm), the two main experimental factors influencing the characteristics of SERS spectra [36]. Since SERS is a surface technique, in a complex mixture such as serum, the binding affinity for the substrate's surface is the main factor determining the SERS features, as the bands of those species with the highest affinity dominate the spectrum. The relative intensity pattern of SERS spectra is shaped by both the adsorption geometry and the difference between excitation wavelength and localised surface plasmons of the metal substrate [1], both of which are likely very similar for all the protocols considered in this study. Although the biochemical interpretation of SERS spectra of serum is still debated, there is a compelling evidence coming from different research groups that, at least when Ag substrates are used with a 785 nm excitation (as in all the protocols considered in this study), most of the bands observed are due to uric acid [7,37], with minor contributions due to other metabolites such as hypoxanthine [7,38] and ergothioneine [39].

By looking data in Fig. 2, apparently the most intense spectra were obtained with protocol 3. However, since laser powers at the sample were different for each protocol, and overall acquisition times varied as well, a direct comparison of absolute intensities is problematic. Protocol 3 has the highest laser power at the sample, and an acquisition time that is longer than protocols 1,4 and 5. Thus, one could object that other protocols could match the intensity of protocol 3 by simply increasing the laser power or acquisition time. However, for those protocols the measurement is performed on a solid sample with a high Ag nanoparticle density (i.e., dried Ag colloids or Ag nanoparticles deposited on paper), whereas for protocol 3 the measurement is performed on a liquid sample (i.e., a drop of Ag colloid mixed with de-proteinized serum). Thus, the use of a higher laser power at the sample or longer acquisition times for the other protocols is limited by the fact that the sample is more susceptible to photothermal degradation, as the heat generated by laser illumination is not dissipated as efficiently as in the liquid phase.

Hence, protocol 3 yielded the most intense spectra also because it

tolerates higher laser powers and longer acquisition times than other protocols. Serum de-proteinization was first introduced by our research group in 2014 [7] when we noticed that the absence of proteins led to intense SERS spectra immediately after adding metal colloids to the sample, interpreting this fact as the hindering of hot-spot formation by the well-known stabilizing effect of protein coronas toward nanoparticles aggregation. The fact that similar SERS spectra could be obtained by prolonged incubation and/or drying by protocols 1 and 2 with whole serum might be due to several reasons. The stabilizing effect of proteins might be waning over time, or the increasing salts concentration upon drying might lead to protein denaturation [40], eventually resulting in the formation of hot-spots. A detailed understanding of the changes in the protein corona structure upon drying is lacking, and its complexity deserves a dedicated investigation, that is, however out of the scope of this study.

Protocols 2 and 4 seem to be less efficient in terms of absolute intensity. Protocol 2, in particular, yielded spectra with a low signal-to-noise ratio in spite of having a relatively high laser power (i.e., 100 mW) and acquisition time (30 s). Varying the laser power did not improve the situation, leading to a lower signal-to-noise ratio (for lower powers) or to sample photodegradation (for higher powers) (data not shown). Also, protocol 2 had the most prominent background signal (Fig. 2A).

When spectra are to be classified in terms of spectral differences reflecting metabolic differences, repeatability of the relative intensity pattern (i.e., overall spectral profile) is usually more important than the repeatability of absolute intensities. Normalized data (Fig. 2C) suggest that protocol 3 presents the lowest variability in the relative intensity pattern, followed by protocols 1 and 5.

A more precise and quantitative comparison of repeatability among the five protocols can be made by looking, for each protocol, at the Euclidean distance of each spectrum from the "median spectrum" (Fig. 3). Smaller distance values reflect a smaller spectral variability calculated over the entire spectrum, confirming that protocol 3 is the most repeatable, while protocols 2 and 4 are the least repeatable.

A further insight on differences among the five protocols can be gathered by analysing the results of a Principal Component Analysis (PCA) in Fig. 4. The scores plot (Fig. 4A) of the two principal components (PC) explain 61 % of the variance (i.e., the spectral variability in

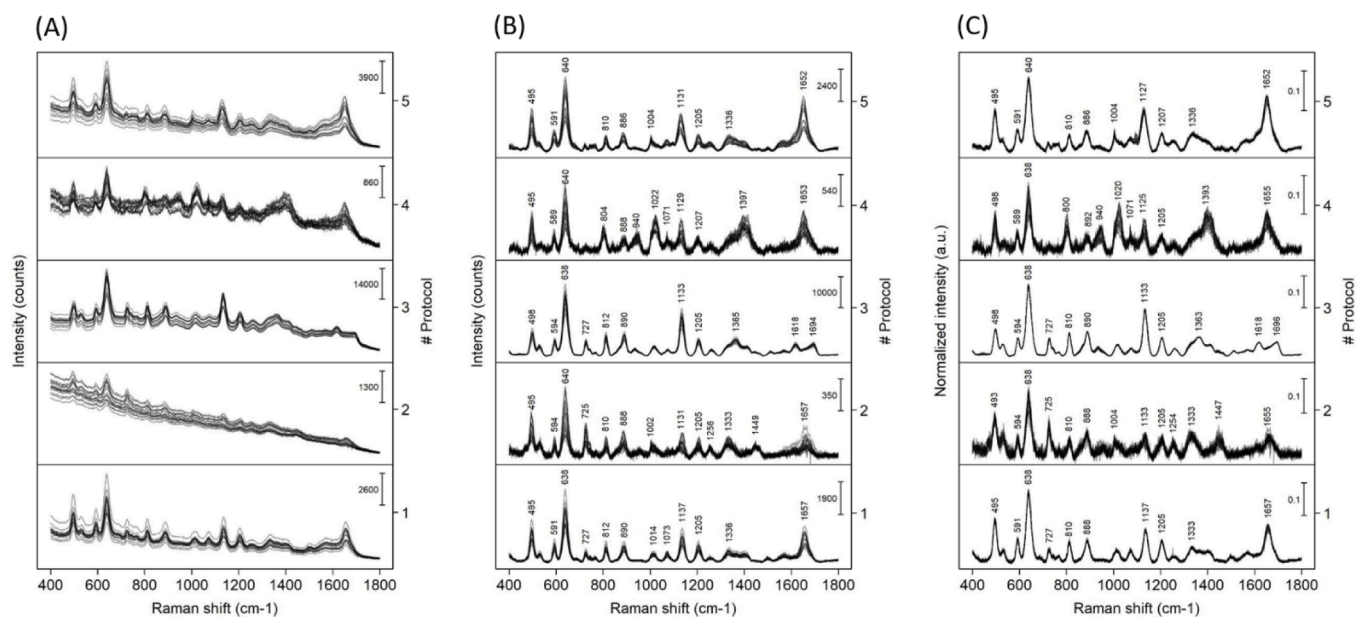


**Fig. 2.** SERS spectra of serum using protocols 1–5 (each row is a different protocol), as described in Materials and Methods: (A) unprocessed spectra, (B) baseline-subtracted spectra, (C) baseline subtracted and intensity normalized spectra. For each protocol, 15 spectra are shown as overlaid, semi-transparent lines. Different intensity scale bars (photon counts) are shown for each set of data on the top right. All spectra were obtained on various Ag substrates, using an excitation at 785 nm.

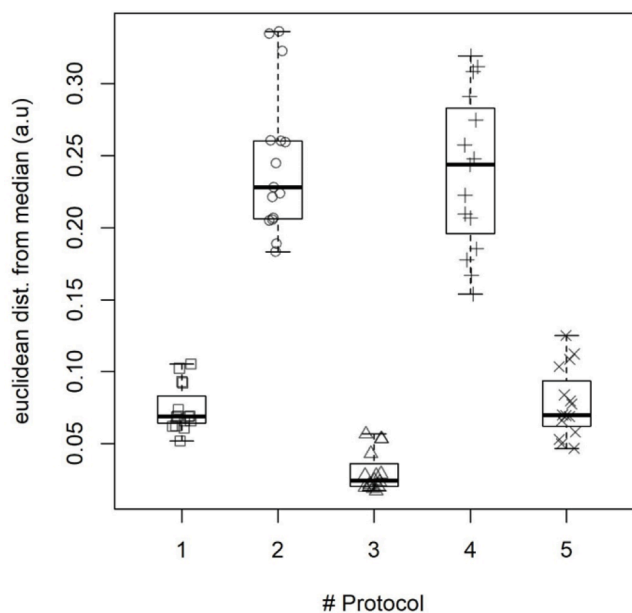


**Fig. 3.** Euclidean distance of each spectrum from the “median spectrum” (calculated as the median of intensity values for each data point over the set of spectra), for protocols 1–5. Each symbol corresponds to a spectrum. Boxplots are added to summarize distribution characteristics.

the dataset), thus confirming that protocol 3 is the one having least variability, as opposed to protocols 2 and 4.

The picture is complemented by the information obtained from the loadings plot (Fig. 4B): the largest variability in the dataset (PC1) is due to a relative intensity difference between bands of uric acid [7] (at 500, 636, 815, 890 and 1135  $\text{cm}^{-1}$ ) and citrate [41] (798, 950, 1024 and 1397  $\text{cm}^{-1}$ ), followed by those between hypoxanthine [7,38] (725, 1449  $\text{cm}^{-1}$ ) and a band at 1650  $\text{cm}^{-1}$  (PC2). PC1 scores and loadings are consistent with the fact that, in protocol 4, a concentrated citrate solution is added to the colloid to promote nanoparticle aggregation on the paper support (positive PC1 loadings match SERS bands of citrate); accordingly, the bands of the other components (mostly uric acid) are

relatively less intense. PC2 suggests that hypoxanthine bands, matching negative PC2 loadings, are most intense in spectra obtained using protocols 2 and 3, whereas a band at 1650  $\text{cm}^{-1}$  is most intense in protocols 1, 4 and 5. Data are insufficient to unequivocally determine the origin of the band at 1650  $\text{cm}^{-1}$ . Its Raman shift is suggestive of a protein amide I band, but the direct SERS detection of amide bands with unmodified citrate-reduced Ag colloids are usually very weak or not observed [42–45]. Moreover, in spectra from samples prepared with protocol 2 (where proteins are present) this band is rather weak, and no positive PC2 loadings are observed where other bands due to protein aromatic residues (e.g., phenylalanine ring breathing mode) would be expected. Also, protocol 3, despite being the only one using de-proteinized serum, has not distinctively different PC1 or PC2 scores (Fig. 4A) from those of other protocols, suggesting that deproteinization does not play a major role in explaining spectral differences among protocols.

However, the scores and loadings of PC3 (Figure S8 – Figure S9), responsible for 19 % of the total variance in the dataset, are suggesting that protein bands might have a role in explaining differences between protocol 3 and other protocols: indeed, negative PC3 loadings are closely resembling Raman spectrum of a protein, and protocol 3 is the one with the highest PC3 scores. However, since all other protocols involve the investigation of a dried sample, where protein concentration is very high, the differences detected by PC3 might be due to the normal Raman scattering of proteins, rather than SERS. Also, PC3 scores show that protocol 2 and 3 are at the opposite extremes, while they have both negative PC2 loadings, indicating that even if negative PC3 loadings can be interpreted as due to proteins, these are not related to the 1650  $\text{cm}^{-1}$  positive features in PC2 loadings plot.

On the other hand, some studies report a band around 1650  $\text{cm}^{-1}$  in SERS spectra of uric acid, whose relative intensity seems to be dependent on experimental conditions such as concentration [46] and electrostatic potential [47]. These data indicate that the overall SERS intensity pattern of uric acid, as it often happens in SERS, varies depending on parameters that might influence the adsorption geometry. Thus, the spectral difference among protocols is depicted by the feature at 1650  $\text{cm}^{-1}$  in the PC2 loadings plot could also be due to an alternative adsorption geometry of uric acid induced by different experimental conditions.

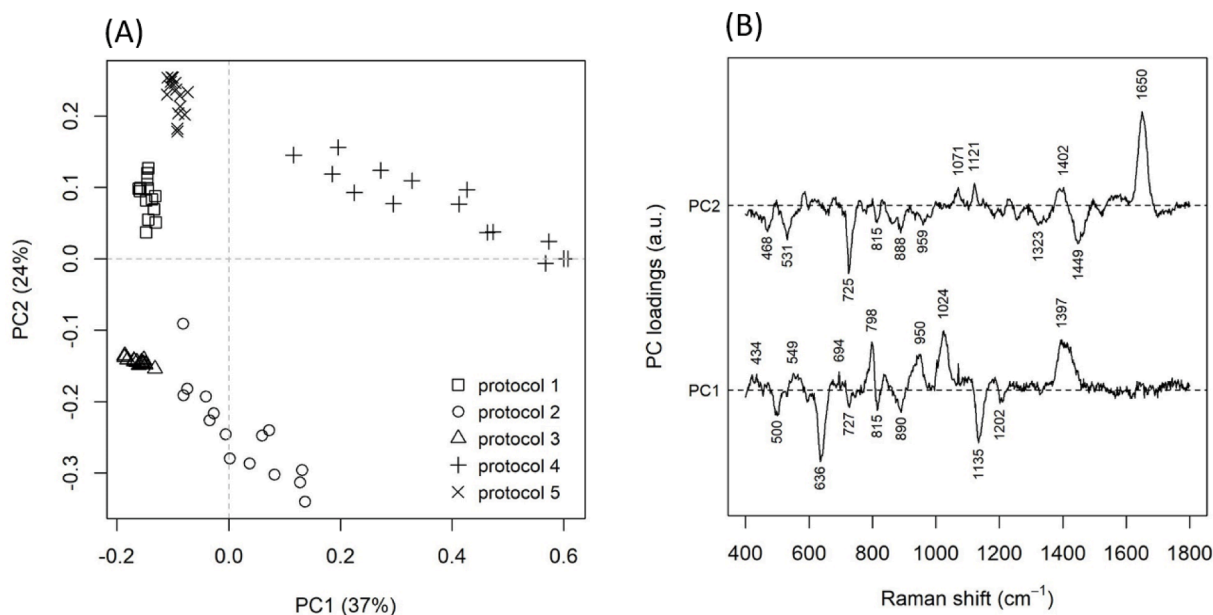


**Fig. 4.** (A) Scores and (B) loadings of principal components (PC) 1 and 2 for the whole spectral dataset (i.e., all spectra from all protocols). In the scores plot (A), each symbol represents one spectrum. In the loadings plot (B), most intense positive and negative values are labelled with the corresponding Raman shift.

#### 4. Conclusions

This direct, controlled comparison among different protocols for a direct SERS analysis of serum shows that all protocols lead to comparable spectra, in terms of overall spectral profile, essentially conveying the same biochemical information. Some protocols (specifically 1, 3 and 5) lead to more repeatable results than others, with protocol 3 being the one with the highest repeatability and signal-to-noise ratio. Serum de-proteinization is beneficial because, by allowing SERS spectra to be rapidly collected from a liquid sample, higher laser powers and acquisition times are well tolerated, and thus spectra with a higher signal-to-noise ratio can be collected. Moreover, de-proteinization does not lead to a significant loss of biochemical information. However, de-proteinization is an additional step, it requires time and also the use of relatively expensive centrifugal filters, at least for the protocol considered in this study. Protocol 1 leads to repeatable spectra with a good signal-to-noise ratio in shorter times, but it requires a colloid concentration step, and a Raman microscope to selectively collect measurements from different spots of the coffee ring region of the dried sample. Protocol 5 is also yielding good results, with the additional advantage that serum samples can be spotted and dried on paper strips, and easily stored/shipped before analysis, although it also requires a centrifugation step for the Ag nanoparticles deposition. Protocol 4 is fast, as it does not involve centrifugation or incubation steps, and only requires the deposition of serum on plasmonic paper before measuring. However, these advantages come at the cost of a lower signal-to-noise ratio and a lower repeatability with respect to other protocols.

#### CRedit authorship contribution statement

**Roberto Gobatto:** Writing – review & editing, Visualization, Investigation. **Stefano Fornasaro:** Writing – review & editing, Visualization, Supervision, Formal analysis. **Valter Sergio:** Writing – review & editing, Supervision, Resources. **Alois Bonifacio:** Writing – original draft, Visualization, Supervision, Formal analysis, Conceptualization.

#### Declaration of competing interest

The authors declare that they have no known competing financial interests or personal relationships that could have appeared to influence the work reported in this paper.

#### Data availability

The dataset and the R code used to produce the figures is openly available on Zenodo (DOI: 10.5281/zenodo.11143059), and can be downloaded from the URL: <https://zenodo.org/records/11143059>.

#### Appendix A. Supplementary material

Supplementary data to this article can be found online at <https://doi.org/10.1016/j.saa.2024.124390>.

#### References

- X. Wang, S.-C. Huang, S. Hu, S. Yan, B. Ren, Fundamental understanding and applications of plasmon-enhanced Raman spectroscopy, *Nat. Rev. Physics* 2 (2020) 253–271, <https://doi.org/10.1038/s42254-020-0171-y>.
- M. Constantinou, K. Hadjigeorgiou, S. Abalde-Cela, C. Andreou, Label-free sensing with metal nanostructure-based surface-enhanced Raman spectroscopy for cancer diagnosis, *ACS Appl. Nano Mater.* 5 (2022) 12276–12299, <https://doi.org/10.1021/acsnm.2c02392>.
- V. Moisoiu, S.D. Iancu, A. Stefanu, T. Moisoiu, B. Pardini, M.P. Dragomir, N. Crisan, L. Avram, D. Crisan, I. Andras, D. Fodor, L.F. Leopold, C. Socaciu, Z. Bálint, C. Tomuleasa, F. Elec, N. Leopold, SERS liquid biopsy: An emerging tool for medical diagnosis, *Colloids Surf. B Biointerfaces* 208 (2021) 112064, <https://doi.org/10.1016/j.colsurfb.2021.112064>.
- N. Psychogios, D.D. Hau, J. Peng, A.C. Guo, R. Mandal, S. Bouatra, I. Sinelnikov, R. Krishnamurthy, R. Eisner, B. Gautam, N. Young, J. Xia, C. Knox, E. Dong, P. Huang, Z. Hollander, T.L. Pedersen, S.R. Smith, F. Bamforth, R. Greiner, B. McManus, J.W. Newman, T. Goodfriend, D.S. Wishart, The human serum metabolome, *PLoS One* 6 (2011) e16957.
- P.C. Lee, D. Meisel, Adsorption and surface-enhanced Raman of dyes on silver and gold sols, *J. Phys. Chem.* 86 (1982) 3391–3395, <https://doi.org/10.1021/j100214a025>.
- N. Leopold, B. Lendl, A new method for fast preparation of highly surface-enhanced Raman scattering (SERS) active silver colloids at room temperature by reduction of silver nitrate with hydroxylamine hydrochloride, *J. Phys. Chem. B* 107 (2003) 5723–5727, <https://doi.org/10.1021/jp027460u>.
- A. Bonifacio, S. Dalla Marta, R. Spizzo, S. Cervo, A. Steffan, A. Colombatti, V. Sergio, Surface-enhanced Raman spectroscopy of blood plasma and serum using Ag and Au nanoparticles: a systematic study, *Anal. Bioanal. Chem.* 406 (2014) 2355–2365, <https://doi.org/10.1007/s00216-014-7622-1>.
- S. Dalla Marta, C. Novara, F. Giorgis, A. Bonifacio, V. Sergio, Optimization and characterization of paper-made surface enhanced Raman scattering (SERS) substrates with Au and Ag NPs for quantitative analysis, *Materials* 10 (2017) 1365, <https://doi.org/10.3390/ma10121365>.
- A. Esposito, A. Bonifacio, V. Sergio, S. Fornasaro, Label-free surface enhanced Raman scattering (SERS) on centrifugal silver plasmonic paper (CSPP): A novel methodology for unprocessed biofluids sampling and analysis, *Biosensors (basel)* 11 (2021) 467, <https://doi.org/10.3390/bios11110467>.
- S. Ahmad, M.I. Majeed, H. Nawaz, M.R. Javed, N. Rashid, M. Abubakar, F. Batool, S. Bashir, M. Kashif, S. Ali, M. Tahira, S. Tabbasum, I. Amin, Characterization and prediction of viral loads of Hepatitis B serum samples by using surface-enhanced Raman spectroscopy (SERS), *Photodiagn. Photodyn. Ther.* 35 (2021) 102386, <https://doi.org/10.1016/j.pdpdt.2021.102386>.
- S. Chen, H. Lin, H. Zhang, F. Guo, S. Zhu, X. Cui, Z. Zhang, Identifying functioning and nonfunctioning adrenal tumors based on blood serum surface-enhanced Raman spectroscopy, *Anal. Bioanal. Chem.* 413 (2021) 4289–4299, <https://doi.org/10.1007/s00216-021-03381-w>.
- S. Gao, Y. Lin, X. Zhao, J. Gao, S. Xie, W. Gong, Y. Yu, J. Lin, Label-free surface enhanced Raman spectroscopy analysis of blood serum via coffee ring effect for accurate diagnosis of cancers, *Spectrochim. Acta A Mol. Biomol. Spectrosc.* 267 (2022) 120605, <https://doi.org/10.1016/j.saa.2021.120605>.
- M. Zong, L. Zhou, Q. Guan, D. Lin, J. Zhao, H. Qi, D. Harriman, L. Fan, H. Zeng, C. Du, Comparison of surface-enhanced Raman scattering properties of serum and urine for the detection of chronic kidney disease in patients, *Appl. Spectrosc.* 75 (2021) 412–421, <https://doi.org/10.1177/0003702820966322>.
- S. Feng, W. Wang, I.T. Tai, G. Chen, R. Chen, H. Zeng, Label-free surface-enhanced Raman spectroscopy for detection of colorectal cancer and precursor lesions using blood plasma, *Biomed. Opt. Express* 6 (2015) 3494, <https://doi.org/10.1364/BOE.6.003494>.
- L. Xia, J. Lu, Z. Chen, X. Cui, S. Chen, D. Pei, Identifying benign and malignant thyroid nodules based on blood serum surface-enhanced Raman spectroscopy, *Nanomedicine* 32 (2021) 102328, <https://doi.org/10.1016/j.nano.2020.102328>.
- S. Chen, S. Zhu, X. Cui, W. Xu, C. Kong, Z. Zhang, W. Qian, Identifying non-muscle-invasive and muscle-invasive bladder cancer based on blood serum surface-enhanced Raman spectroscopy, *Biomed. Opt. Express* 10 (2019) 3533, <https://doi.org/10.1364/BOE.10.003533>.
- Y. Lu, Y. Lin, Z. Zheng, X. Tang, J. Lin, X. Liu, M. Liu, G. Chen, S. Qiu, T. Zhou, Y. Lin, S. Feng, Label free hepatitis B detection based on serum derivative surface enhanced Raman spectroscopy combined with multivariate analysis, *Biomed. Opt. Express* 9 (2018) 4755, <https://doi.org/10.1364/BOE.9.004755>.
- D. Lin, Y. Wang, T. Wang, Y. Zhu, X. Lin, Y. Lin, S. Feng, Metabolite profiling of human blood by surface-enhanced Raman spectroscopy for surgery assessment and tumor screening in breast cancer, *Anal. Bioanal. Chem.* 412 (2020) 1611–1618, <https://doi.org/10.1007/s00216-020-02391-4>.
- R. Zhu, Y. Jiang, Z. Zhou, S. Zhu, Z. Zhang, Z. Chen, S. Chen, Z. Zhang, Prediction of the postoperative prognosis in patients with non-muscle-invasive bladder cancer based on preoperative serum surface-enhanced Raman spectroscopy, *Biomed. Opt. Express* 13 (2022) 4204, <https://doi.org/10.1364/BOE.465295>.
- B.A. Buhas, V. Toma, N. Crisan, G. Ploussard, T.A. Maghiar, R.-I. Știufiuc, C. M. Lucaciu, High-accuracy renal cell carcinoma discrimination through label-free SERS of Blood serum and multivariate analysis, *Biosensors (basel)* 13 (2023) 813, <https://doi.org/10.3390/bios13080813>.
- C. Pan, K. Peng, T. Chen, G. Chen, Y. Lin, Q. Zhang, M. Liu, D. Lin, T. Wang, S. Feng, Power-Law-based synthetic minority oversampling technique on imbalanced serum surface-enhanced Raman spectroscopy data for cancer screening, *Adv. Intell. Syst.* 5 (2023), <https://doi.org/10.1002/aisy.202300006>.
- S. Peng, D. Lu, B. Zhang, R. You, J. Chen, H. Xu, Y. Lu, Machine learning-assisted internal standard calibration label-free SERS strategy for colon cancer detection, *Anal. Bioanal. Chem.* 415 (2023) 1699–1707, <https://doi.org/10.1007/s00216-023-04566-1>.
- F. Gao, D.-C. Lu, T.-L. Zheng, S. Geng, J.-C. Sha, O.-Y. Huang, L.-J. Tang, P.-W. Zhu, Y.-Y. Li, L.-L. Chen, G. Targher, C.D. Byrne, Z.-F. Huang, M.-H. Zheng, Fully connected neural network-based serum surface-enhanced Raman spectroscopy accurately identifies non-alcoholic steatohepatitis, *Hep. Intl.* 17 (2023) 339–349, <https://doi.org/10.1007/s12072-022-10444-2>.
- Q. Zhang, Y. Chen, X. Zou, W. Hu, X. Lin, S. Feng, F. Chen, L. Xu, W. Chen, N. Wang, Prognostic analysis of amyotrophic lateral sclerosis based on clinical features and plasma surface-enhanced Raman spectroscopy, *J. Biophotonics* 12 (2019), <https://doi.org/10.1002/jbio.201900012>.
- X. Zheng, G. Wu, J. Wang, L. Yin, X. Lv, Rapid detection of hystero myoma and cervical cancer based on serum surface-enhanced Raman spectroscopy and a

- support vector machine, *Biomed. Opt. Express* 13 (2022) 1912, <https://doi.org/10.1364/BOE.448121>.
- [26] M. Tahira, H. Nawaz, M.I. Majeed, N. Rashid, S. Tabbasum, M. Abubakar, S. Ahmad, S. Akbar, S. Bashir, M. Kashif, S. Ali, H. Hyat, Surface-enhanced Raman spectroscopy analysis of serum samples of typhoid patients of different stages, *Photodiagn. Photodyn. Ther.* 34 (2021) 102329, <https://doi.org/10.1016/j.pdpdt.2021.102329>.
- [27] S. Li, L. Li, Q. Zeng, Y. Zhang, Z. Guo, Z. Liu, M. Jin, C. Su, L. Lin, J. Xu, S. Liu, Characterization and noninvasive diagnosis of bladder cancer with serum surface enhanced Raman spectroscopy and genetic algorithms, *Sci. Rep.* 5 (2015) 9582, <https://doi.org/10.1038/srep09582>.
- [28] H. Li, S. Zhang, R. Zhu, Z. Zhou, L. Xia, H. Lin, S. Chen, Early assessment of chemotherapeutic response in hepatocellular carcinoma based on serum surface-enhanced Raman spectroscopy, *Spectrochim. Acta A Mol. Biomol. Spectrosc.* 278 (2022) 121314, <https://doi.org/10.1016/j.saa.2022.121314>.
- [29] C.-C. Xiong, S.-S. Zhu, D.-H. Yan, Y.-D. Yao, Z. Zhang, G.-J. Zhang, S. Chen, Rapid and precise detection of cancers via label-free SERS and deep learning, *Anal. Bioanal. Chem.* 415 (2023) 3449–3462, <https://doi.org/10.1007/s00216-023-04730-7>.
- [30] W. Dawuti, J. Dou, J. Li, R. Zhang, J. Zhou, M. Maimaitiaili, R. Zhou, R. Lin, G. Lü, Label-free surface-enhanced Raman spectroscopy of serum with machine-learning algorithms for gallbladder cancer diagnosis, *Photodiagn. Photodyn. Ther.* 42 (2023) 103544, <https://doi.org/10.1016/j.pdpdt.2023.103544>.
- [31] A. Bonifacio, S. Cervo, V. Sergio, Label-free surface-enhanced Raman spectroscopy of biofluids: fundamental aspects and diagnostic applications, *Anal. Bioanal. Chem.* 407 (2015) 8265–8277, <https://doi.org/10.1007/s00216-015-8697-z>.
- [32] E. Gurian, A. Di Silvestre, E. Mitri, D. Pascut, C. Tiribelli, M. Giuffrè, L.S. Crocè, V. Sergio, A. Bonifacio, Repeated double cross-validation applied to the PCA-LDA classification of SERS spectra: a case study with serum samples from hepatocellular carcinoma patients, *Anal. Bioanal. Chem.* 413 (2021) 1303–1312, <https://doi.org/10.1007/s00216-020-03093-7>.
- [33] R Core Team, R: A language and environment for statistical computing. R Foundation for Statistical Computing, (2020). <https://www.R-project.org/>.
- [34] Claudia Beleites, Valter Sergio, "hyperSpec: a package to handle hyperspectral data sets in R," (n.d.). <https://github.com/cbeleites/hyperSpec>.
- [35] K.H. Liland, T. Almøy, B.-H. Mevik, Optimal choice of Baseline Correction for Multivariate Calibration of Spectra, *Appl. Spectrosc.* 64 (2010) 1007–1016, <https://doi.org/10.1366/000370210792434350>.
- [36] H. Fisk, C. Westley, N.J. Turner, R. Goodacre, Achieving optimal SERS through enhanced experimental design, *J. Raman Spectrosc.* 47 (2016) 59–66, <https://doi.org/10.1002/jrs.4855>.
- [37] E. Avci, H. Yilmaz, N. Sahiner, B.G. Tuna, M.B. Cicekdal, M. Eser, K. Basak, F. Altintoprak, I. Zengin, S. Dogan, M. Çulha, Label-free surface enhanced Raman spectroscopy for cancer detection, *Cancers (basel)* 14 (2022) 5021, <https://doi.org/10.3390/cancers14205021>.
- [38] W.R. Premasiri, J.C. Lee, L.D. Ziegler, Surface-enhanced Raman scattering of whole human blood, blood plasma, and red blood cells: cellular processes and bioanalytical sensing, *J. Phys. Chem. B* 116 (2012) 9376–9386, <https://doi.org/10.1021/jp304932g>.
- [39] S. Fornasaro, E. Gurian, S. Pagarin, E. Genova, G. Stocco, G. Decorti, V. Sergio, A. Bonifacio, Ergothioneine, a dietary amino acid with a high relevance for the interpretation of label-free surface enhanced Raman scattering (SERS) spectra of many biological samples, *Spectrochim. Acta A Mol. Biomol. Spectrosc.* 246 (2021) 119024, <https://doi.org/10.1016/j.saa.2020.119024>.
- [40] C. Cantarutti, Y. Hunashal, C. La Rosa, M. Condorelli, S. Giorgetti, V. Bellotti, F. Fogolari, G. Esposito, The corona of protein–gold nanoparticle systems: the role of ionic strength, *PCCP* 24 (2022) 1630–1637, <https://doi.org/10.1039/D1CP04574A>.
- [41] L. Marsich, A. Bonifacio, S. Mandal, S. Krol, C. Beleites, V. Sergio, Poly-L-lysine-coated silver nanoparticles as positively charged substrates for surface-enhanced Raman scattering, *Langmuir* 28 (2012) 13166–13171, <https://doi.org/10.1021/la302383r>.
- [42] P.-S. Wang, H. Ma, S. Yan, X. Lu, H. Tang, X.-H. Xi, X.-H. Peng, Y. Huang, Y.-F. Bao, M.-F. Cao, H. Wang, J. Huang, G. Liu, X. Wang, B. Ren, Correlation coefficient-directed label-free characterization of native proteins by surface-enhanced Raman spectroscopy, *Chem. Sci.* 13 (2022) 13829–13835, <https://doi.org/10.1039/D2SC04775F>.
- [43] D. Li, Z. Zhang, X. Wang, Y. Wang, X. Gao, Y. Li, A direct method for detecting proteins in body fluids by Surface-Enhanced Raman Spectroscopy under native conditions, *Biosens. Bioelectron.* 200 (2022) 113907, <https://doi.org/10.1016/j.bios.2021.113907>.
- [44] Y. Bao, Y. Li, L. Ling, X. Xiang, X. Han, B. Zhao, X. Guo, Label-free and highly sensitive detection of native proteins by Ag IANPs via surface-enhanced Raman spectroscopy, *Anal. Chem.* 92 (2020) 14325–14329, <https://doi.org/10.1021/acs.analchem.0c03165>.
- [45] C. Zong, M. Xu, L.-J. Xu, T. Wei, X. Ma, X.-S. Zheng, R. Hu, B. Ren, Surface-enhanced Raman spectroscopy for bioanalysis: reliability and challenges, *Chem. Rev.* 118 (2018) 4946–4980, <https://doi.org/10.1021/acs.chemrev.7b00668>.
- [46] Y. Lu, C. Wu, R. You, Y. Wu, H. Shen, L. Zhu, S. Feng, Superhydrophobic silver film as a SERS substrate for the detection of uric acid and creatinine, *Biomed. Opt. Express* 9 (2018) 4988, <https://doi.org/10.1364/BOE.9.004988>.
- [47] B.L. Goodall, A.M. Robinson, C.L. Brosseau, Electrochemical-surface enhanced Raman spectroscopy (E-SERS) of uric acid: a potential rapid diagnostic method for early preeclampsia detection, *PCCP* 15 (2013) 1382–1388, <https://doi.org/10.1039/C2CP42596C>.